

CHAPTER 4.3

A NEW LEUKOENCEPHALOPATHY
WITH BRAINSTEM AND
SPINAL CORD INVOLVEMENT
AND HIGH LACTATE

Marjo S. van der Knaap
Patrick van der Voorn
Frederik Barkhof
Rudy Van Coster
Ingeborg Krägeloh-Mann
Annette Feigenbaum
Susan Blaser
Johan S.H. Vles
P. Rieckmann
Petra J. W. Pouwels

Ann Neurol. 2003 Feb;53(2):252-8

ABSTRACT

We identified eight patients with a distinct MRI pattern of inhomogeneous cerebral white matter abnormalities and selective involvement of brainstem and spinal tracts. Proton MRS showed increased lactate in the abnormal white matter. Clinically the patients had slowly progressive pyramidal, cerebellar and dorsal column dysfunction. The uniform, highly characteristic MRI pattern and the similarities in clinical and MRS findings provide evidence for a new disease entity. Autosomal recessive inheritance is likely.

INTRODUCTION

White matter disorders of unknown etiology constitute a considerable problem in childhood¹. MRI and MRS have been used to identify “new” diseases among them. In two MRI-defined disorders, megalencephalic leukoencephalopathy with subcortical cysts² and vanishing white matter³, the gene defects have recently been identified⁴⁻⁶, confirming the value of this MRI-oriented approach.

We describe a novel distinct MRI pattern, shared by eight patients. Apart from cerebral and cerebellar white matter abnormalities, striking findings are the involvement of specific brainstem and spinal cord tracts and elevated lactate in the abnormal white matter. These findings are paralleled by a homogeneous clinical presentation, reinforcing the concept of a new syndrome.

PATIENTS AND METHODS

In all patients except patient 8, at least the last study was performed on the same 1.5 T MRI machine. The protocol included brain and spinal MRI, and short-echo time proton MRS of volumes of mid-parietal cortex (8 ml) and abnormal white matter in the centrum semiovale (5 ml), as described previously⁷. Metabolite concentrations, calculated with LCModel in mmol/l⁸, were compared with results of 12 controls (age range 9.3-26.3) using the two-tailed unpaired student T-test.

Diffusion tensor imaging (DTI) and magnetization transfer (MT) imaging were performed in patients 1-7 and 12 controls. For DTI a multi-slice EPI sequence was used⁹. Mean diffusivity, $\langle D \rangle$, and fractional anisotropy (FA) were calculated^{9,10} for the same white matter and cortex volumes as selected for MRS. MT imaging was performed with a 3D-FLASH sequence. MT ratio (MTR) maps were obtained from pairs of identical images acquired with and without MT saturation pulse. Mean MTR was calculated for again the same volumes. The DTI and MTR results of patients and controls were compared using the one-tailed unpaired student T-test.

RESULTS

Clinical profiles and laboratory examinations

Neurological deterioration started in childhood or adolescence (table 1). Spasticity and ataxia affected legs more than arms. Patients 1 and 2 are presently wheelchair-dependent and have severely decreased manual dexterity. Patients 3, 5, 6 and 7 have a spastic-ataxic gait, but can still walk unsupported and have moderately decreased manual dexterity.

Table. Clinical History and Findings

Characteristic	Patient							
	1	2	3	4	5	6	7	8
Gender	Female	Female	Female	Male	Female	Female	Male	Male
Year of birth	1967	1979	1982	1983	1984	1987	1992	1992
Affected/unaffected siblings	0/0	1/0 (Patient 3)	1/0 (Patient 2)	0/1	0/1	1/0 (Patient 7)	1/0 (Patient 6)	0/1
Consanguinity of parents	—	—	—	—	—	—	—	? (adopted)
Initial motor development	n	n	n	n	n	n	n	?
Unsupported walking (mo)	15, always unstable	14, always unstable	15	14	15	16, always unstable	24, always unstable	?, unstable
Onset of motor deterioration (yr)	5	3	5	6	15	7	—	—
Loss of unsupported walking (yr)	14	14	—	—	—	—	—	—
Dysarthria	+	+	—	—	—	—	+	—
Motor signs of arms								
Tone	n	↓	↓	n	n	n	n	n
Reflexes	n	↑	n	n	n	n	↑	n
Ataxia	++	++	+	+	+	+	+	+
Strength	↓ in hands	↓ in hands	n	n	n	↓ in hands	n	n
Motor signs of Legs								
Tone	↑ ↑	↑ ↑	n	Distal ↑	Distal ↑	n	n	n
Reflexes	n	↑	↑	↑ ↑	↑ ↑	n	↑	↑
Babinski signs	+	+	+	+	+	+	+	—
Ataxia	Not testable	++	+	+	+	+	++	+
Strength	Serious spastic paresis	Serious spastic paresis	Mild spastic paresis	Subtle spastic paresis	Mild spastic paresis	Mild spastic paresis	Mild spastic paresis	n
Sensory function	Distal ↓ in position and vibration sense	n	n	n	Distal ↓ in position and vibration sense	Distal ↓ in position and vibration sense	Distal ↓ in position and vibration sense	n
Bladder function	Incontinence	n	n	n	n	n	n	n
Vision, hearing	n	n	n	n	n	n	n	n
Intelligence	n	Learning problems	n	n	Learning problems	Learning problems	n	Learning problems
Cognitive decline	—	—	—	—	—	—	—	—
Epilepsy	—	—	—	—	1 seizure	—	—	1 seizure
No. of MRIs/age range (yr)	2/32–34	5/16–22	5/13–20	3/15–18	7/8–18	3/6–14	3/2–10	2/7–8

n = normal; mo = months; yr = years; + = present; ++ = serious; ↓ = decrease; ↓ ↓ = serious decrease; ↑ = increase; ↑ ↑ = serious increase.

Patients 4 and 8 show mild abnormalities on neurological examination but have no functional problems. Four patients have a distal decrease in position and vibration sense. Four patients have learning problems.

The following laboratory investigations were performed in all or multiple patients and unrevealing: in blood hematology and chemistry panels, blood gases, ammonia, creatine kinase, cholesterol, vitamin E, vitamin B₁₂, folic acid, thyroid function, karyotype, amino acids, lactate, pyruvate, very long-chain fatty acids, phytanic acid, transferrin isoelectric focusing, carnitine, copper, ceruloplasmin, cholestanol, and lysosomal enzymes (arylsulfatase-A, galactocerebrosidase, beta-galactosidase and hexosaminidase-A); in urine organic acids, oligosaccharides, purines, pyrimidines, sialic acid and sulfatides; in CSF cell count, protein and lactate. Analysis of mitochondrial function in fresh mitochondria from muscle and mitochondrial DNA did not reveal abnormalities.

Somatosensory evoked potentials with stimulation of tibial and median nerves, obtained in five patients, were delayed in four and absent in one. Sensory and motor nerve conduction velocities (six patients) were normal. Sural nerve biopsy revealed no abnormalities in patient 4.

Magnetic Resonance

Thirty brain MRIs were obtained (for ages see table 1). The full-blown pattern consisted of extensive signal changes within the periventricular and deep cerebral white matter, relatively or completely sparing the temporal lobes and the U-fibers throughout (Fig. 1, 2). There was some increase in extent over time in three of the patients. The signal changes were inhomogeneous with a spotty aspect. The spots had a lower signal intensity on FLAIR images suggesting focal rarefaction³. The posterior corpus callosum was always affected; the anterior part was not involved or less seriously. The posterior limb of the internal capsule was abnormal. The cerebellar white matter became involved later, initially in the subcortical regions (Fig. 1d) and subsequently diffusely (Fig. 2d). The oldest patient had some cerebellar atrophy. Within the brainstem, the superior and inferior cerebellar peduncles were involved early, whereas the middle cerebellar peduncles became affected in a late stage. Within the midbrain, the pyramidal tracts and medial lemniscus were abnormal. Within the pons, the structures typically involved were the pyramidal tracts, medial lemniscus, intraparenchymal trajectories of the trigeminal nerves and mesencephalic trigeminal tracts. In late stages, the transverse pontine fibers became abnormal. Within the medulla, signal changes were typically present in the pyramids, medial lemniscus, inferior cerebellar peduncles and anterior spinocerebellar tracts. After contrast (two patients) no enhancement was found.

The clinical severity correlated with the severity of disease on brain MRI. Patient 4 had the mildest clinical picture and MRI abnormalities; patient 1 had the most severe clinical symptoms and MRI abnormalities.

Fifteen spinal MRIs were obtained. They showed abnormalities in the dorsal columns and lateral corticospinal tracts uniformly over the entire length in all patients (Fig. 1). There were no changes on follow-up. There was no evident atrophy.

White matter $\langle D \rangle$ was significantly higher in patients (mean $1.07 \times 10^{-3} \text{ mm}^2/\text{s}$; s.d. 0.30) than in controls (mean $0.81 \times 10^{-3} \text{ mm}^2/\text{s}$, s.d. 0.07). However, there was a considerable variability and in some patients $\langle D \rangle$ was normal. The increase in cortical $\langle D \rangle$ was also significant but less pronounced ($1.07 \times 10^{-3} \text{ mm}^2/\text{s}$, s.d. 0.05 in patients; $0.94 \times 10^{-3} \text{ mm}^2/\text{s}$, s.d. 0.03 in controls). White matter FA was significantly lower in patients (mean 0.22, s.d. 0.04) than in controls (mean 0.37, s.d. 0.04), while cortical FA was normal (mean 0.17, s.d. 0.01 in patients; mean 0.18, s.d. 0.01 in controls). MTR was significantly lower in the white matter of patients (mean 20.5%, s.d. 2.8) than controls (mean 31.8%, s.d. 1.5), and normal in the cortex (mean 24.6%, s.d. 1.5 in patients; mean 25.4%, s.d. 1.2 in controls).

In MRS a significant decrease in N-acetylaspartate (NAA) and increase in myo-inositol (mIns) were found in the white matter of patients (mean NAA 4.6 mmol/l, s.d. 0.8; mean mIns 5.9 mmol/l, s.d. 0.7) as compared to controls (mean NAA 7.7 mmol/l, s.d. 1.0; mean mIns 3.6 mmol/l, s.d. 0.3). The increase in white matter choline (Cho) was also statistically significant, but less pronounced (in patients mean 1.8 mmol/l, s.d. 0.3; in controls mean 1.3 mmol/l; s.d. 0.2). White matter creatine (Cr) was normal (in patients

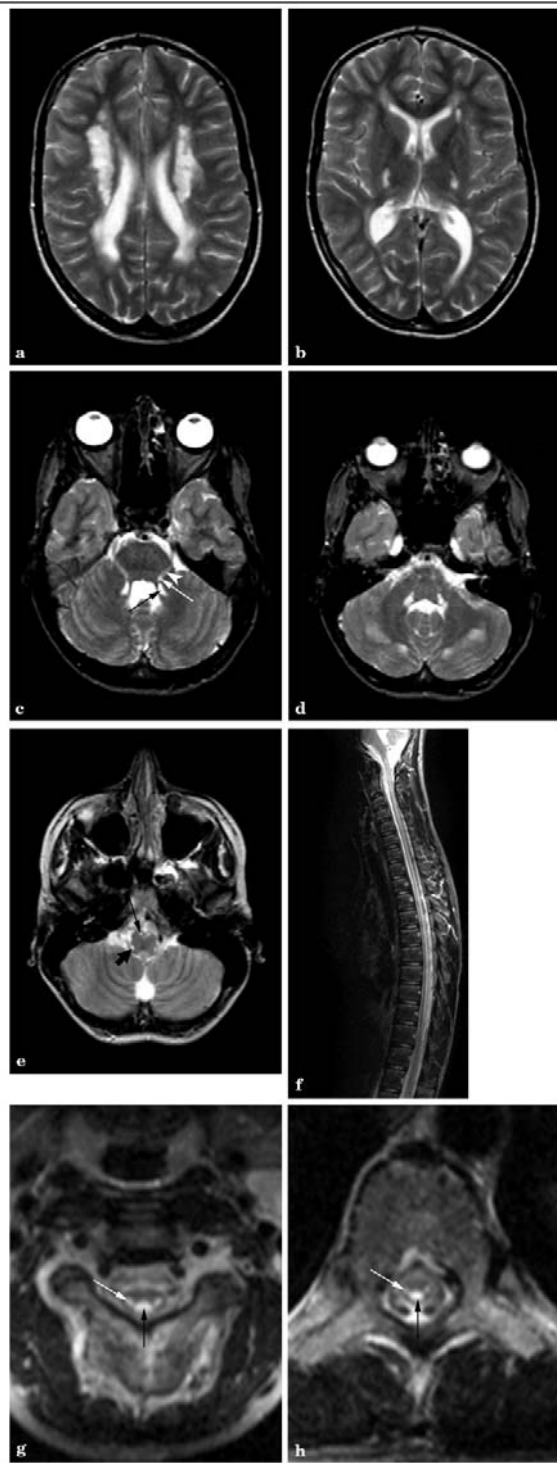


Figure 1 shows T2-weighted images of the brain (a - e) and spinal cord (f - h) in patient 6. There are irregular, spotty signal abnormalities in the periventricular white matter (a, b), extending into the posterior limb of the internal capsule (b). Within the brainstem, the intraparenchymal trajectories of the trigeminal nerves (arrow head in c), the mesencephalic trigeminal tracts (white arrow in c), the superior cerebellar peduncles (black arrow in c), the inferior cerebellar peduncles (bold arrow in e) and the pyramids (small arrow in e) are involved. The subcortical cerebellar white matter contains signal abnormalities (d). The sagittal spinal image (f) shows that the cord contains signal abnormalities over its entire length. Transverse images at the cervical (g) and thoracic (h) levels show that the dorsal columns (black arrow) and lateral corticospinal tracts (white arrow) have an abnormal signal. The low signal behind the spinal cord (h) represents flow artefacts.

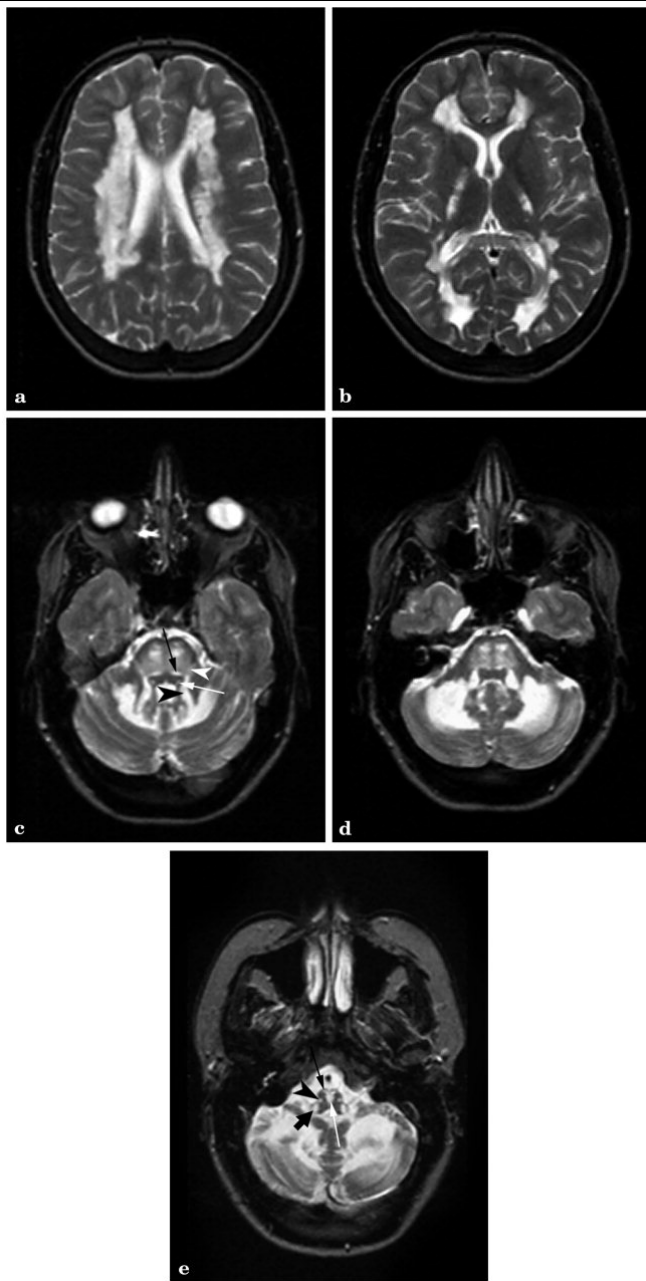


Figure 2 shows the corresponding images in the more severely affected patient 3. The periventricular white matter changes have an inhomogeneous, spotty appearance (a,b). The posterior part of the corpus callosum is more severely involved than the anterior part (b). The posterior limb of the internal capsule is abnormal. Within the brainstem, the intraparenchymal trajectories of the trigeminal nerves (white arrow head in c), the mesencephalic trigeminal tracts (white arrow in c), medial lemniscus (black arrow in c, white arrow in e), pyramidal tracts (c), transverse pontine fibers (c), superior cerebellar peduncles (black arrow head in c), inferior cerebellar peduncles (bold black arrow in e), pyramids (small black arrow in e), and anterior spinocerebellar tracts (arrow head in e) are abnormal in signal. All white matter of the cerebellar hemispheres is abnormal (d).

mean 4.6 mmol/l, s.d. 0.8; in controls mean 4.5 mmol/l, s.d. 0.6). White matter lactate was elevated in all patients except one (mean 2.4 mmol/l, range 0.5-4.1, s.d. 1.1; in controls 0.2 mmol/l, s.d. 0.3). MRS of white matter in patient 8 in another center showed increased lactate. Cortical spectra were normal.

DISCUSSION

Definition of the syndrome

A novel leukoencephalopathy is described. It is clinically characterized by slowly progressive pyramidal and cerebellar dysfunction, often with concomitant dorsal column dysfunction. The MRI pattern is distinct and includes inhomogeneous cerebral white matter abnormalities and strikingly selective tract involvement. The pyramidal tracts extending downwards through the internal capsule and the brainstem into the lateral corticospinal tracts are affected over their entire length. The sensory tracts, including dorsal columns, medial lemniscus up to the level of the thalamus, and corona radiata above that level are also affected over their entire length. Cerebellar connections are selectively involved. The consistent involvement of the intraparenchymal trajectories of the trigeminal nerve and mesencephalic trigeminal tracts is remarkable. This MRI pattern is uniform among the patients and different from patterns in both classical and recently defined leukoencephalopathies^{2,3,11}. It does not resemble the pattern of pontocerebellar atrophy observed in the familial spinocerebellar ataxias¹² or the white matter changes observed in some hereditary spastic paraparesis syndromes¹³. At present the diagnosis is MRI-based and requires the presence of typical spinal cord abnormalities in combination with spotty cerebral white matter abnormalities and specific brainstem abnormalities.

Pathophysiology

MRI is very sensitive in detecting white matter abnormalities but lacks specificity with respect to underlying pathology. Other MR techniques may contribute in this respect. In MRS, the abnormal cerebral white matter showed normal to mildly elevated Cho concentrations, suggesting low-grade demyelination¹⁴. The decrease in NAA and increase in mIns were more pronounced, indicating considerable axonal damage or loss¹⁵ and gliosis¹⁶, respectively. Gliosis can contribute to Cho elevations¹⁷. DTI and MTR provide information about tissue microstructure. Within the abnormal white matter of our patients, $\langle D \rangle$, a measure for isotropic water diffusivity, was increased in most, whereas FA, a measure for the degree of diffusion anisotropy, was decreased in all; these changes indicate an enhanced mobility of water molecules in all directions as a result of damage to the tissue matrix¹⁸. The MTR of the abnormal white matter was decreased, probably reflecting loss of axons¹⁹ and myelin sheaths²⁰.

Overall, our findings suggest considerable axonal damage or loss in the white matter. The involvement of entire tracts argues in favor of primary axonal degeneration.

There is an element of myelin loss, which could be secondary. It is difficult to explain the early discrepancy between MRI abnormalities and clinical problems. At present the pathologic basis of the disease remains unsolved.

Extensive laboratory investigations did not reveal a cause. Considering the presence of two affected sib-pairs among our patients, an autosomal recessive mode of inheritance is likely. We will initiate a genetic linkage study as soon as sufficient informative families are available.

ACKNOWLEDGEMENTS

We thank Drs. M. Cercignani, and M. Filippi from the Neuroimaging Research Unit, University of Milan, Italy, and Dr. M.A. Horsfield, Division of Medical Physics, University of Leicester, UK, for providing us with the pulse sequence and post-processing software for diffusion tensor imaging. Dr. J.M. Powers, Department of Pathology, University of Rochester Medical Center, Rochester NY, is acknowledged for critical reading of the manuscript.

REFERENCES

1. Van der Knaap MS, Breiter SN, Naidu S, Hart AAM, Valk J. Defining and categorizing leukoencephalopathies of unknown origin: MR imaging approach. *Radiology* 1999; 213: 121-133.
2. Van der Knaap MS, Barth PG, Stroink H, van Nieuwenhuizen O, Arts WFM, Hoogenraad F, Valk J. Leukoencephalopathy with swelling and a discrepantly mild clinical course in eight children. *Ann Neurol* 1995; 37: 324-334.
3. Van der Knaap MS, Barth PG, Gabreëls FJM, Franzoni E, Begeer JH, Stroink H, Rotteveel JJ, Valk J. A new leukoencephalopathy with vanishing white matter. *Neurology* 1997; 48: 845-855.
4. Leegwater PAJ, Yuan BQ, van der Steen J, Mulders J, Könst AAM, Boor PKI, Mejaski-Bosnjak V, van der Maarel SM, Frants RR, Oudejans CBM, Schutgens RBH, Pronk JC, van der Knaap MS. Mutations of MLC1 (KIAA0027), encoding a putative membrane protein, cause megalencephalic leukoencephalopathy with subcortical cysts. *Am J Hum Genet* 2001; 68: 831-838.
5. Leegwater PAJ, Vermeulen G, Könst AAM, Naidu S, Mulders J, Visser A, Kersbergen P, Mobach D, Fonds D, van Berkel CGM, Lemmers RJLF, Frants RR, Oudejans CBM, Schutgens RBH, Pronk JC, van der Knaap MS. Subunits of the translation initiation factor eIF2B are mutated in leukoencephalopathy with vanishing white matter. *Nature Genet* 2001; 29: 383-388.
6. Van der Knaap MS, Leegwater PAJ, Könst AAM, Visser A, Naidu S, Oudejans CBM, Schutgens RBH, Pronk JC. Mutations in each of the five subunits of translation initiation factor eIF2B can cause leukoencephalopathy with vanishing white matter. *Ann Neurol* 2002; 51: 264-270.
7. Van der Knaap MS, Wevers RA, Struys EA, Verhoeven NM, Pouwels PJW, Engelke UFH, Feikema W, Valk J, Jakobs C. Leukoencephalopathy associated with a disturbance in the metabolism of polyols. *Ann Neurol* 1999; 46: 925-928.
8. Provencher SW. Estimation of metabolite concentrations from localized in vivo proton MR spectra. *Magn Reson Med* 1993; 30: 672-679.
9. Jones DK, Horsfield MA, Simmons A. Optimal strategies for measuring diffusion in anisotropic systems by magnetic resonance imaging. *Magn Reson Med* 1999; 42: 515-525.
10. Basser PJ, Pierpaoli C. Microstructural and physiological features of tissues elucidated by quantitative-diffusion-tensor MRI. *J Magn Reson B* 1996; 111: 209-219.
11. Van der Knaap MS, Valk J. *Magnetic resonance of myelin, myelination and myelin disorders*. Heidelberg, Springer, 1995.
12. Higgins JJ, Harvey-White JD, Nee LE, Colli MJ, Grossi TA, Kopin I. Brain MRI, lumbar CSF monoamine concentrations, and clinical descriptors of patients with spinocerebellar ataxia mutations. *J Neurol Neurosurg Psychiatry* 1996; 61: 591-595.
13. Fukazawa T, Sasaki H, Kikuchi S, Hamada K, Hamada T, Tashiro K. Dominantly inherited leukodystrophy showing cerebellar deficits: a new entity? *J Neurol* 1997; 244: 446-449.
14. Davie CA, Hawkins CP, Barker GJ, Brennan A, Tofts PS, Miller DH, McDonald WI. Serial proton magnetic resonance spectroscopy in acute multiple sclerosis lesions. *Brain* 1994; 117: 49-58.

15. Simmons ML, Frondoza CG, Coyle JT. Immunocytochemical localization of N-acetylaspartate with monoclonal antibodies. *Neuroscience* 1991; 45: 37-45.
16. Brand A, Richter-Landsberg C, Leibfritz D. Multinuclear NMR studies on the energy metabolism of glial and neuronal cells. *Dev Neurosci* 1993; 15: 289-298
17. Bitsch A, Bruhn H, Vougioukas V, Stringaris A, Lassmann H, Frahm J, Brück W. Inflammatory CNS demyelination: histopathologic correlation with in vivo quantitative proton MR spectroscopy. *American Journal of Neuroradiology* 1999; 20: 1619-1627
18. Filippi M, Cercignani M, Inglese M, Horsfield MA, Comi G. Diffusion tensor magnetic resonance imaging in multiple sclerosis. *Neurology* 2001; 56: 304-311
19. Van Waesberghe JHTM, Kamphorst W, de Groot CJA, van Walderveen MAA, Castelijns JA, David R, Lycklama à Nijeholt GJ, van der Valk P, Polman CH, Thompson AJ, Barkhof F. Axonal loss in multiple sclerosis lesions: magnetic resonance imaging insights into substrates of disability. *Ann Neurol* 1999; 46: 747-754
20. Deloire MSA, Brochet B, Quesson B, Delalande C, Dousset V, Canioni P, Petry KG. In vivo evaluation of remyelination in rat brain by magnetization transfer imaging. *J Neurol Sci* 2000; 178: 10-16